Dynamic Flexibility of a Peptide-Binding Groove of Human HLA-DR1 Class II MHC Molecules: Normal Mode Analysis of the Antigen Peptide–Class II MHC Complex

Hiroyuki NOJIMA,[a] Mayuko TAKEDA-SHITAKA,[a] Youji KURIHARA,[a] Kenshu KAMIYA,[b] and Hideaki UMEYAMA*,[a]

[a] *School of Pharmaceutical Sciences, Kitasato University; 5–9–1 Shirokane, Minato-ku, Tokyo 108–8641, Japan: and* [b] *School of Science, Kitasato University; 1–15–1 Sagamihara, Kanagawa 228–8555, Japan.*
Received February 21, 2003; accepted May 8, 2003

Class II major histocompatibility complex (MHC) has tolerance for binding longer antigen peptides than those bound by class I MHC. In this paper, a normal mode analysis on HLA-DR1 class II MHC involving an antigen peptide indicated that the peptide-binding groove had some different dynamic characteristics from that of HLA-A2 class I MHC. The dynamic changes in the class I groove with removal of the bound peptide were limited primarily to the central region and the C-terminal side (corresponding to the C-terminal side of the bound peptide) of the groove, while the dynamic changes in the class II groove with removal of the bound peptide extended to the whole of the groove, and were especially remarkable around a strand located in the N-terminal side (corresponding to the N-terminal side of the bound peptide) of the groove. These results suggest that the N-terminal side of the class II groove is more flexible than the same side of the class I groove, and this flexibility may allow some N-terminal residues of the bound peptide to extend outside the class II groove. Definite anti-correlative motions with removal of the bound peptide appeared between two α-helical regions of class II MHC as in the case of class I MHC. These motions of the class II groove may play an important role in obtaining "a flexible dynamic fit" against diverse longer peptides both of whose terminals extend outside the groove.

Key words class II major histocompatibility complex; peptide-binding groove; normal mode analysis; anti-correlative motion

Class II major histocompatibility complex (MHC) is a cell-surface protein, which engages an antigen peptide in the endosomal compartments of antigen-presenting cells for the stimulation of T cells as activators of an immune response.[1,2] Class II MHC is composed of an asymmetric dimer (α-chain: 182 residues, and β-chain: 190 residues), and although domain organizations are different from those of class I MHC (α-chain: 275 residues, and β-chain: 100 residues), three-dimensional structures are roughly similar to those of class I MHC, with two membrane-proximal immunoglobulin-like domains, an eight-stranded β-sheet and a peptide-binding groove formed by two α-helical regions.[3—6] In the engagement of an antigen peptide with a MHC, it is a common characteristic of both class I and class II MHCs that their peptide-binding grooves bind to antigen peptides with diverse sequences. However, the class I groove binds to peptides of limited length (usually 8—10 residues), while the class II groove has the capacity to bind to longer peptides (8—23 residues, usually 14 to 15 residues on average).[7—13] Stern *et al.* compared the X-ray structure of HLA-DR1 class II MHC with that of HLA-A2 class I MHC and indicated that the peptide-binding style of the class II groove was different from that of the class I groove,[6] but this difference has not provided a clear reason why only class II MHC is able to bind to longer peptides.

On the other hand, Bouvier and Wiley[14] and Nakagawa *et al.*[15] indicated that the peptide-binding groove after dissociation of the bound peptide becomes unstable as the temperature increases compared with other domains of MHC. Their reports may support the importance of the dynamics of MHC for peptide-binding, especially the dynamic characteristics of the groove formed by the two α-helical regions. Previously, we performed a normal mode analysis on HLA-A2 class I MHC involving three antigen peptides with different affinities, and found some dynamic changes in the groove with removal of the bound peptide.[16] Therefore, comparison of a normal mode analysis on class II MHC with that on class I MHC may provide some different dynamic characteristics between the two classes of II MHC. In this study, we performed normal mode analyses on HLA-DR1 class II MHC involving the antigen peptide derived from influenza virus hemagglutinin (13 residues: HA 306—318 (PKYVKQNTLKLAT); called the HA peptide) and HLA-A2 class I MHC involving the antigen peptide derived from HTLV-1 Tax protein (9 residues: Tax 11—19 (LLFGYPVYV); called the Tax peptide).[5,6] On each MHC, a normal mode analysis of MHC involving an antigen peptide (the complexed structure) and MHC alone (the peptide-removed structure) was performed. In both structures, fluctuations and motional correlation coefficients were calculated, and the characteristics that distinguish class II MHC from class I MHC are discussed from a dynamic point of view.

Results

Fluctuation Changes in the Peptide-Binding Groove with Removal of the Antigen Peptides In both HLA-A2 class I and HLA-DR1 class II MHCs, the fluctuation patterns of all frequency modes were very similar to those in the low frequency modes below 50 cm^{-1}, and definite fluctuation changes with removal of the bound peptide were not found in high frequency modes over 50 cm^{-1} (data not shown). In this study, the number of low frequency modes below 50 cm^{-1} ranged from 131 to 144 for class I MHC, and from 146 to 161 for class II MHC. The ratio of the low frequency modes to total modes was *ca.* 8.0—8.8% for class I MHC, and *ca.* 9.1—10.5% for class II MHC. Class II MHC has different domain organizations from class I MHC, but showed roughly similar fluctuation patterns. This similarity reflects their

* To whom correspondence should be addressed. e-mail: umeyamah@pharm.kitasato-u.ac.jp

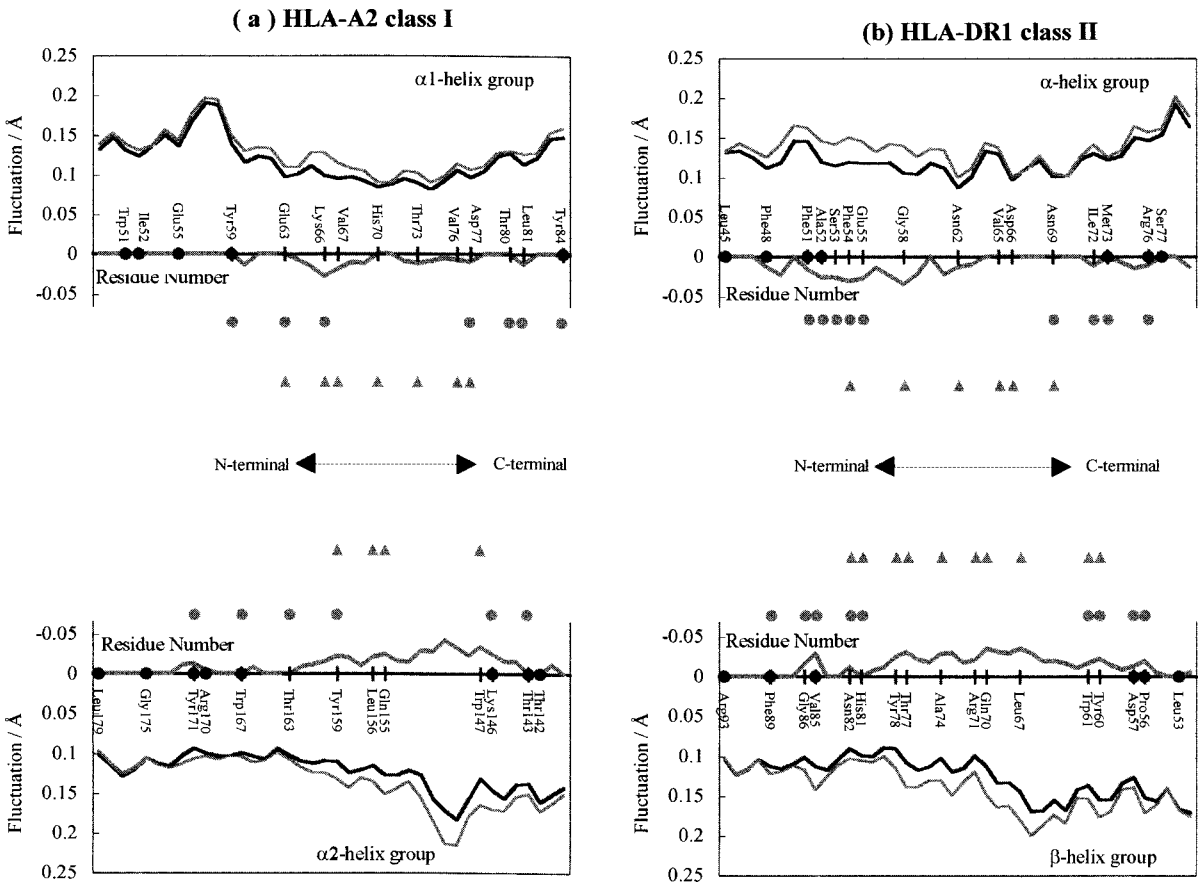

Fig. 1. Cα Atom Fluctuations of the Two Helix Groups in the Low Frequency Modes below 50 cm^{-1}

Above are fluctuations in the α1-helix group (or the α-helix group), and below are fluctuations in the α2-helix group (or the β-helix group). In each figure, the left side corresponds to the N-terminal side of the bound peptide and the right side corresponds to the C-terminal side of the peptide. The black and gray lines show fluctuations in the complexed and peptide-removed structures, respectively. Significant differences by Wilcoxon's rank sum test are shown by thick gray lines. A zero value indicates "no significant difference" by Wilcoxon's rank sum test. The black circles on the zero line show that the corresponding residues are close to the opposite helix group (<4 Å). (a) HLA-A2 class I MHC. The gray circles show that the corresponding residues are close to the N-terminal residue (Leu11) or the C-terminal residue (Val19) of the Tax peptide (<4 Å). The gray triangles indicate that the corresponding residues are close to the central region (-LFGYPVY-) of the Tax peptide (<4 Å). (b) HLA-DR1 class II MHC, the gray circles that the corresponding residues are close to the N-terminal residues (Pro306–Lys307–Tyr308) or the C-terminal residues (Leu316–Ala317–Thr318) of the HA peptide (<4 Å). The gray triangles show that the corresponding residues are close to the central region (-VKQNTLK-) of the HA peptide (<4 Å).

three-dimensional structures rather than their domain organizations. Definite fluctuation changes with removal of the bound peptide were not found except in the two α-helical regions.

The α-chain of HLA-A2 class I MHC has two α-helical regions which form a peptide-binding groove (residues α-49—84 in the α1-domain [called the α1-helix group] and residues α-140—179 in the α2-domain [the α2-helix group]), while in HLA-DR1 class II MHC, each α- and β-chain has one α-helical region (residues α-45—79 in the α1-domain [the α-helix group] and residues β-52—93 in the β1-domain [the β-helix group]), which form a peptide-binding groove. The Cα atom fluctuations of the peptide-binding groove were compared between class I and class II MHCs (Fig. 1). With removal of the bound peptide, the class II groove showed peculiar fluctuation changes that were different from those of the class I groove.

The α1-helix group of class I MHC (Fig. 1a, above) showed a fluctuation peak at residues α-57—58, which are located near a kink (α-Glu55 and α-Gly56). Fluctuation changes in the α1-helix group with removal of the Tax peptide were found at the right side of the peak (residues α-64—69, α-72—77), which is close to the central region (Leu12–Tyr18) of the Tax peptide. On the other hand, the α-helix group of class II MHC (Fig. 1b, above) has a strand structure (residues α-52—56), which is not seen in the α1-helix group of class I MHC. Fluctuation changes in the α-helix group with removal of the HA peptide were found around the strand (residues α-48—49, α-51—59, α-61—63), which is close to the N-terminal side and the central region (Pro306–Thr308) of the HA peptide.

The α2-helix group of class I MHC (Fig. 1a, below) showed a fluctuation peak at residues α-149—150, which form a kink (α-Ala149 and α-Ala150). Fluctuation changes in the α2-helix group with removal of the Tax peptide were arranged around the kink (residues α-144—162), which is close to the C-terminal side (Val19) and the central region (Leu12–Tyr18) of the Tax peptide. The β-helix group of class II MHC (Fig. 1b, below) also showed a fluctuation peak at residues β-65—66 which are located near a kink (β-Ser63 and β-Gln64). Fluctuation changes in the β-helix group with removal of the HA peptide were ranged widely around the kink (residues β-55—79), which is close to the C-terminal side (Leu316–Ala317) and the central region (Val309–Lys315) of the HA peptide. In addition, residues β-85—86 of the β-helix group showed large fluctuation changes which

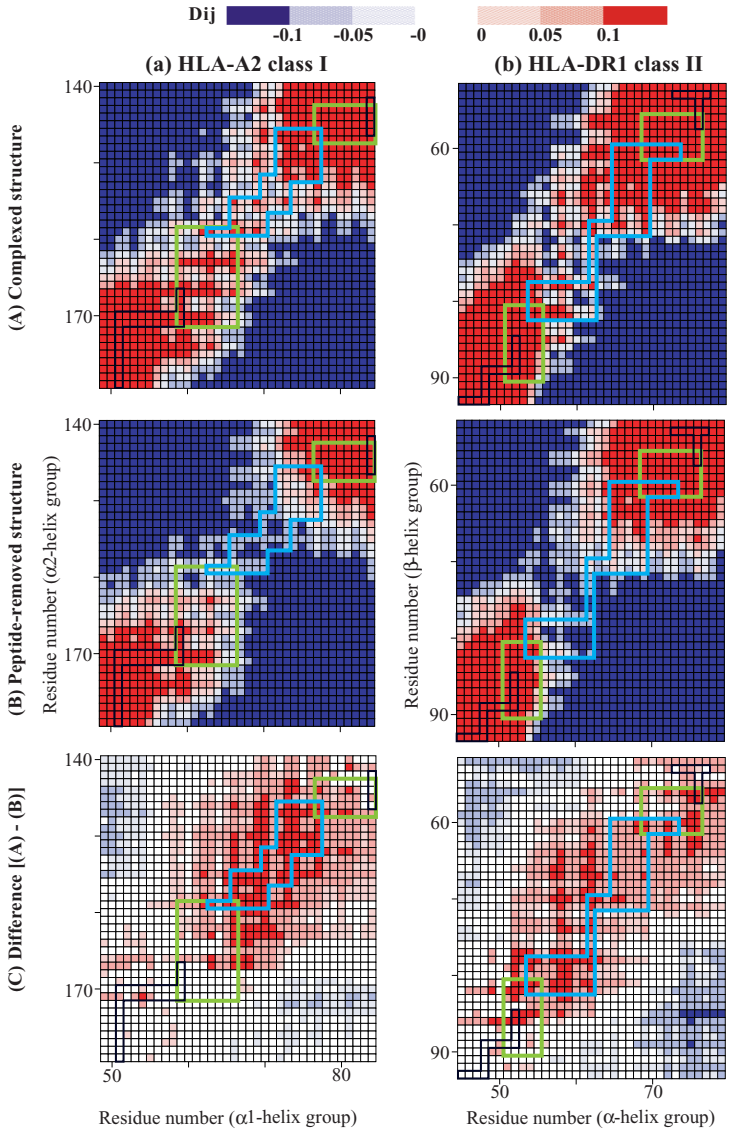

Fig. 2. Motional Correlation Coefficient Maps of the Cα Pairs between the Two Helix Groups in the Low Frequency Modes below 50 cm^{-1}

The profiles of motional correlation coefficients of the Cα pairs between the two helix groups in the low frequency modes below 50 cm^{-1} were similar to those in the total frequency modes. In each map, the Cα pairs on the lower left correspond to the N-terminal side of the bound peptide and those on the upper right correspond to the C-terminal side of the peptide. The upper (A) and middle (B) lines show the complexed and peptide-removed structures, respectively. In both lines, the positive (Dij>0) and negative (Dij<0) correlation coefficients are shown in red and blue, respectively. The deeper the colors, the higher the absolute values. The lower line (C) shows significant differences between the structures [(A)—(B)]. If the Dij in the complexed structure is significantly different from the Dij in the peptide-removed structure by Wilcoxon's rank sum test, the matrix is in color. Red shows where the difference [Dij (A)—(B)] is positive (>0), blue shows where the difference is negative (<0), and no color means the difference is not significant by Wilcoxon's rank sum test. The black frames include the residue pairs close to each other (<4 Å). Left line (a): HLA-A2 class I MHC. The green frames include the residue pairs "close to" the N-terminal residue (Leu11) or the C-terminal residue (Val19) of the Tax peptide. The cyan frames include the residue pairs "close to" the central region (-LFGYPVY-) of the Tax peptide (<4 Å). Here, "close to" means that the average of {the shortest distance (PA) between a residue (P) in the bound peptide−a residue (A) in one-side helix group} and {the shortest distance (PB) between the residue (P)−a residue (B) in the opposite-side helix group}, that is [(PA+PB)/2], is shorter than 4 Å. Right line (b): HLA-DR1 class II MHC. The green frames include the residue pairs "close to" the N-terminal residues (Pro306–Lys307–Tyr308) or the C-terminal residues (Leu316–-Ala317–Thr318) of the HA peptide (<4 Å). The cyan frames include the residue pairs "close to" the central region (-VKQNTLK-) of the HA peptide (<4 Å).

participate in the binding of the N-terminal side (Pro306–Tyr308) of the HA peptide.

Motional Correlation Changes in the Peptide-Binding Groove with Removal of the Antigen Peptides Motional correlation coefficient maps of Cα pairs between the two helix groups of HLA-DR1 class II MHC were compared with those of HLA-A2 class I MHC (Fig. 2). A positive correlation means the corresponding Cα pair moves in roughly the same direction, while a negative correlation means that it moves in roughly the opposite direction. In the complexed structure (A), the map of the class I groove (upper left in Fig. 2) showed positive correlation coefficients along a diagonal from the lower left to the upper right. The Cα pairs along the diagonal are closer to each other than the other Cα pairs in between the two helix groups. With removal of the Tax peptide (B), the center of the map (middle left in Fig. 2) showed negative changes in the correlation coefficients.

The map profiles of the class II groove (upper right and middle right in Fig. 2) were roughly similar to those of the class I groove in both structures, but significant differences between the structures clearly showed a peculiar behavior of the class II groove that was different from the class I groove. The correlative changes [(A)—(B)] in the class I groove were gathered on the center and upper right of the map (lower left

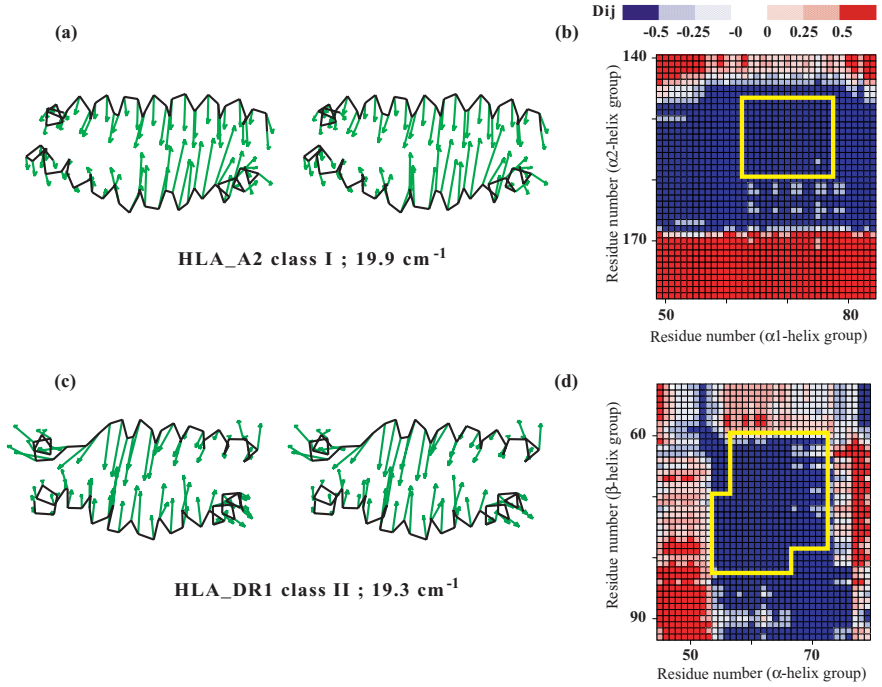

Fig. 3. Examples of Definite Anti-correlative Motions in the Peptide-Removed Structure

At left are stereo drawings of the Cα atomic displacement vectors of the two helix groups. The displacement vectors are multiplied by 1000. At right are their maps of motional correlation coefficients. Positive (Dij>0) and negative (Dij<0) correlation coefficients are shown in red and blue, respectively. The deeper the colors, the higher the absolute values, but note that the color range of the maps is different from that of the maps in Fig. 2. In the case of HLA-DA2 class I MHC, the definite anti-correlative motions were decided by the ratio (over 92%) of the Cα pairs that show a negative correlation coefficient (cos θ<−0.5) of the 195 Cα pairs in the yellow frame (Fig. 3b). In the case of HLA-DR1 class II MHC, the definite anti-correlative motions were decided by the ratio (over 78%) of the Cα pairs that show a negative correlation coefficient (cos θ<−0.5) of the 383 Cα pairs in the yellow frame (Fig. 3d). (a), (b) One example of definite anti-correlative motions of HLA-A2 class I MHC. (c), (d) One example of definite anti-correlative motions of HLA-DR1 class II.

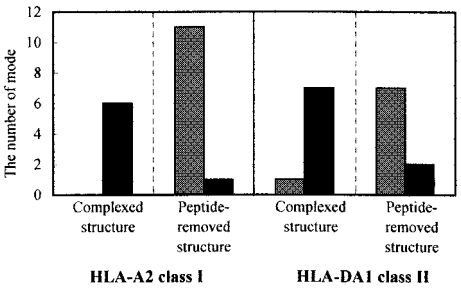

Fig. 4. The Number of Definite Anti-correlative and Correlative Motions

The gray and black bars indicate definite anti-correlative and correlative motions, respectively. In the case of HLA-A2 class I MHC, the definite anti-correlative and correlative motions were decided by the ratio (over 92%) of the Cα pairs that show negative (cos θ<−0.5) and positive (cos θ>0.5) correlation coefficients of the 195 Cα pairs in the yellow frame (see Fig. 3b). In the case of HLA-DR1 class II MHC, the definite anti-correlative and correlative motions were decided by the ratio (over 78%) of the Cα pairs that show negative (cos θ<−0.5) and positive (cos θ>0.5) correlation coefficients of the 383 Cα pairs in the yellow frame (Fig. 3d).

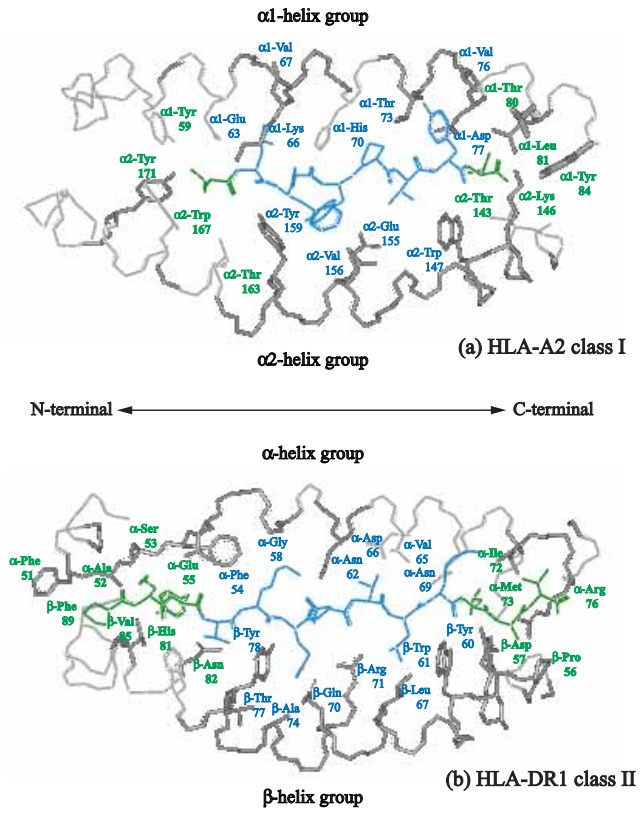

Fig. 5. Drawings of HLA-A2 Class I and HLA-DR Class II Peptide-Binding Grooves

In each figure, the left side corresponds to the N-terminal side of the bound peptide and the right side corresponds to the C-terminal side of the peptide. The main chain (N-Cα-C) of the two helix groups and some side chains close to the antigen peptide (<4 Å: with residue number) are drawn. Residues whose fluctuations are changed with removal of the antigen peptide are drawn with a stick, and in them, residues that are close to the bound peptide (<4 Å) are labeled. (a) HLA-A2 class I MHC. The green residue labels show that the corresponding residues are close to the N-terminal residue (Leu11) or the C-terminal residue (Val19) of the Tax peptide. The blue residue labels show that the corresponding residues are close to the central region (-LFGYPVY-) of the Tax peptide (<4 Å). (b) HLA-DR1 class II MHC. The green residue labels show that the corresponding residues are close to the N-terminal residues (Pro306–Lys307–Tyr308) or the C-terminal residues (Leu316–Ala317–Thr318) of the HA peptide (<4 Å). The blue residue labels show that the corresponding residues are close to the central region (-VKQNTLK-) of the HA peptide (<4 Å).

in Fig. 2). This field corresponds to the central region and the C-terminal side of the groove (corresponding to the C-terminal side of the Tax peptide) close to most of the Tax peptide, except for the N-terminus (NH_3^+) and C-terminus (COO^-). On the other hand, the correlative changes [(A)—(B)] in the class II groove extended from the lower left to the upper right of the map (lower right in Fig. 2). This field corresponds to the whole of the groove close to most of the HA peptide (PKYVKQNTLKLA-), except for the C-terminal residue (Thr 318).

Anti-correlative and Correlative Motions between the Two Helix Groups Previously, in HLA-A2 class I MHC, we found that negatively correlated motions (named anti-correlative motions) appeared between the two helix groups in the low frequency modes below 50 cm^{-1} with removal of the bound peptide.[16] In the class I MHC of this study, anti-correlative motions also appeared between the two helix groups with removal of the Tax peptide. The motion, as shown in Fig. 3a, has negatively correlated (correlation coefficient<-0.5) residue pairs over 92% of the 195 Cα pairs at the center of the map [in the yellow rectangular frame in Fig. 3b]. The above definite motion was not found in any of the six optimized complexed structures, but 11 modes appeared in all of the six optimized peptide-removed structures (Fig. 4). In HLA-DR1 class II MHC, similar anti-correlative motions between the two helix groups were also found in the low frequency modes below 50 cm^{-1}. The motion, as shown in Fig. 3c, which has negatively correlated (correlation coefficient<-0.5) residue pairs over 78% of the 383 Cα pairs at the center of the map [in the yellow frame in Fig. 3d]. The above definite motion was only one mode in all of the six optimized complexed structures, but 7 modes appeared in all of the six optimized peptide-removed structures (Fig. 4).

Discussion

The class II peptide-binding groove, which is formed by the two helix groups, has roughly similar three-dimensional structures to the class I peptide-binding groove.[3—6] However, some crystal structures of class II MHC involving an antigen peptide indicate that the peptide-binding style of the class II groove is different from that of the class I groove.[6,9,13] In order to bind to an antigen peptide, the class I groove needs primarily to accommodate the N- (NH_3^+) and C- (COO^-) termini of the bound peptide.[5,17—19] On this occasion, longer peptides (10 residues) usually zigzag or bulge to allow themselves to maintain the relative positions of both termini.[5,20—22] In addition, the class I groove has some specific pockets primarily composed of polymorphic residues, which accommodate some amino acid side chains of the bound peptide, termed anchors.[10,11,23,24] The class II groove forms many hydrogen bonds between its conserved residues and the main chain of the bound peptide, and has five pockets to accommodate the side chains of the bound peptide.[6,9,13] In the five pockets, both edges are deeper than the other pockets and important for binding to the peptide. Nine amino acids in a peptide bound to class II MHC are generally located between the above-mentioned edges, and therefore the edges may play roles similar to the pockets of the class I groove that accommodate both termini of the bound peptide. However, the peptides bound to class II MHC neither zigzag nor bulge like peptides bound to class I MHC, but twist and extend from of both ends of the class II groove.[6,9,13] Why, then, does the class II groove allow the binding of longer peptides than those bound to the class I groove?

The normal mode analyses in this study offer some information with respect to this question. A normal mode analysis on HLA-A2 class I MHC involving the Tax peptide indicated that the dynamic changes in the class I groove with removal of the Tax peptide were primarily gathered at the central region and the C-terminal side (corresponding to the C-terminal side of the Tax peptide) of the groove, and that the dynamic changes in the N-terminal side (corresponding to the N-terminal side of the Tax peptide) were slight (Fig. 5a). This result was similar to the report when we performed the normal mode analysis on HLA-A2 class I MHC involving other three antigen peptides.[16] The slight dynamic change in the N-terminal side is believed to be because of the dense packing of the three aromatic side chains (α-Tyr59, α-Trp167 and α-Tyr171) even when the Tax peptide was removed. This side probably needs to be hard in order to form the strict electrostatic interaction of a pocket with the N-terminus (NH_3^+) of the bound peptide. The relation between the N-terminus of the bound peptide and the pocket is similar to the "key and keyhole", seen in many enzyme-substrate interactions. On the other hand, the normal mode analysis on HLA-DR1 class II MHC indicated that the dynamic changes in the class II groove with removal of the HA peptide extended to the whole of the groove (Fig. 5b). The remarkable change in the class II groove was found around a strand (residues α-52—56) located in the N-terminal side (corresponding to the N-terminal side of the HA peptide). The strand, which has no large side chain, is not found in the N-terminal side of the class I groove.[6,9,13] The remarkable change may be due to hollowing out of the vacant space of the N-terminal side with removal of the HA peptide. This result suggests that the N-terminal side of the class II groove is more flexible than the same side of the class I groove, and that this flexibility may allow some N-terminal residues of the bound peptide to extend outside the class II groove. The N-terminal residues (Pro306 and Lys307) of the HA peptide are located outside the class II groove, but probably contribute to stabilization of the peptide-binding.

The C-terminal side of the class I groove has a few different dynamic changes from the N-terminal side (Fig. 5a). This side is packed by two aromatic side chains (α-Tyr84 and α-Trp147) and accommodates the C-terminal residue of the peptide. However, residues α-144—162 in the α2-helix group showed large dynamic changes with removal of the Tax peptide. This result may arise because the C-terminal side is flexible due to a kink (α-Ala150 and α-Ala151). Class I MHC is able to bind some peptides with 10 residues, and one of the binding-modes allows the C-terminus (COO^-) of the bound peptide to extend outside the groove. This is seen for the signal sequence peptide derived from calreticulin.[23,25] Thus, the C-terminal side of the class I groove may show more flexible behavior than the N-terminal side of the class I groove. The β-helix group of class II MHC also has a kink (β-Ser53 and β-Gln54) at a similar position to the α2-helix group of class I MHC (Fig. 5b), and residues β-56—80 in the β-helix group showed large dynamic changes when removing the HA peptide. The C-terminal side of the class II groove (corresponding to the C-terminal side of the HA pep-

tide) may also be flexible because of the kink. In addition, Ala 317 of the HA peptide, which is located out of the class II groove, probably contributes to stabilization of the peptide binding.

Generally, the dynamic characteristics of proteins are heavily influenced by low frequency modes.[26] In the low frequency modes ($<50\,cm^{-1}$), anti-correlative motions between the two helix groups of both the MHCs appeared with removal of the bound peptide. The appearance of definite anti-correlative motions, as shown in Fig. 4, reflects the difference in correlation distribution in the low frequency modes ($<50\,cm^{-1}$) between the complexed and peptide-removed structures. For both the MHCs, the definite anti-correlative motions may play a similar role in obtaining a "dynamic fit" against antigen peptides with diverse sequences. However, the dynamic changes in connection with the appearance of the definite anti-correlative motions are limited primarily to the central region of the class I groove, while those changes are extended to the whole of the class II groove. These results suggest that the definite anti-correlative motions of the class II groove play an important role in obtaining "a flexible dynamic fit" against longer peptides both of whose terminals extended outside the class II groove.

Experimental

Protein Structures X-ray structures of HLA-DR1 class II MHC involving the HA peptide, and HLA-A2 class I MHC involving the Tax peptide, were obtained from the Brookhaven Protein Data Bank (PDB; PDB code 1DLH,[6] and 1HHK[5]). In the PDB of HLA-DR1, the A-chain of 176 residues (residues 5—180) as the α-chain, the B-chain of 186 residues (residues 5—190) as the β-chain, and the C-chain of 13 residues (HA: residues 306—318) as the HA peptide, were used in the calculations for the complexed structure. In the PDB of HLA-A2, the D-chain of 275 residues (residues 1—275) as the α-chain, the E-chain of 100 residues (residues 0—99) as the β-chain, and the F-chain of 9 residues (Tax: residues 11—19) as the Tax peptide, were used in the calculations for the complexed structure. The A and B chains of HLA-DR1 and the D and E chains of HLA-A2 were taken as each peptide-removed structure, and were used in these calculations.

Normal Mode Analysis The energy optimization was performed with a slightly modified AMBER united atom force field,[27] and the normal mode analysis was performed with torsion angles. In the AMBER force field, parameters of bond angles and dihedral angles including disulfide bonds were removed because a suspected potential was imposed, which treats disulfide bonds as a function of the distance between S–S atoms and does not explicitly consider disulfide bond angles and dihedral angles. The energy optimization and normal mode analysis were calculated by programs which were developed by our laboratory.[28,29] For our calculations, we assumed that the molecules were *in vacuo*, but a distance-dependent dielectric constant (r/Å) for the electrostatic energy was maintained.[30] The electrostatic potential and the van der Waals potential were cut off at 9.0 Å, and were switched smoothly and continuously to a value of zero at 10.0 Å. A bond energy was imposed on the X-ray structure in the geometric optimization process and the restriction was gradually relaxed so that the normal mode analysis was executed near the experimental coordinates including water molecules. A threshold of 0.04 kcal/mol Å for the maximal component of gradients of atoms was used. The structure was in a local energy-minimum state near the X-ray structure in the energy landscape. Six energetically optimized structures in both the peptide-removed and complexed structures were obtained under various conditions of restriction about each peptide-MHC complex. Normal mode analysis was carried out for these optimized structures. In this study, the total number of modes about class II MHC was 1603 in the complexed structure and 1538 in the peptide-removed structure, and that about HLA-A2 class I MHC was 1672 in the complexed structure and 1635 in the peptide-removed structure. Fluctuations in Cα atoms and motional correlation coefficients between the Cα pairs were calculated using our program assuming a temperature of 300 K.[31—33] The fluctuations and correlation coefficients in the peptide-removed and complexed structures were determined by averaging those of the six optimized structures. Under Eckart's conditions,[34] the fluctuations and correlation coefficients of the MHC inner motions in the complexed structure were compared with those in the peptide-removed structure. To subtract the fluctuations and correlation coefficients in the peptide-removed structure from those in the complexed structure, significant differences were estimated by Wilcoxon's rank sum test, a nonparametric test.

References

1) Germain R. N., Margulies D. H., *Annu. Rev. Immunol.*, **11**, 403—450 (1993).
2) Jorgensen J. L., Reay P. A., Ehrivh E. W., Davis M. M., *Annu. Rev. Immunol.*, **10**, 835—873 (1992).
3) Bjorkman P. J., Saper M. A., Samraoui B., Bennett W. S., Strominger J. L., Wiley D. C., *Nature* (London), **329**, 506—512 (1987).
4) Brown J. H., Jardetzky T. S., Gorga J. C., Stern L. J., Urban R. G., Strominger J. L., Wiley D. C., *Nature* (London), **364**, 33—39 (1993).
5) Madden D. R., Garboczi D. N., Wiley D. C., *Cell*, **75**, 693—708 (1993).
6) Stern L. J., Brown J. H., Jardetzky T. S., Gorga J. C., Urban R. G., Strominger J. L., Wiley D. C., *Nature* (London), **368**, 215—221 (1994).
7) Chicz R. M., Urban R. G., Lane W. S., Gorga J. C., Stern L. J., Vignali D. A., Strominger J. L., *Nature* (London), **358**, 764—768 (1992).
8) Falk K., Rötzschke O., Stevanoić S., Jung G., Rammensee H.-G., *Nature* (London), **351**, 290—296 (1991).
9) Gosh P., Amaya M., Mellins E., Wiley D. C., *Nature* (London), **378**, 457—462 (1995).
10) Hunt D. F., Henderson R. A., Shabanowitz J., Sakaguchi K., Michel H., Sevilir N., Cox A. L., Appella E., Engelhard V. H., *Science*, **255**, 1261—1263 (1992).
11) Jardetzky T. S., Lane W. S., Robinson R. A., Madden D. R., Wiley D. C., *Nature* (London), **353**, 326—329 (1991).
12) Matsumura M., Fremont D. H., Peterson P. A.,Wilson I. A., *Science*, **257**, 927—934 (1992).
13) Murthy V. L., Stern L. J., *Structure*, **5**, 1385—1396 (1997).
14) Bouvier M., Wiley D. C., *Nature Struct. Biol.*, **5** 377—384 (1998).
15) Nakagawa M., Chiba-Kamoshida K., Udaka K., Nakanishi H., *Biochem. Biophys. Res. Commun.*, **278**, 609—613 (2000).
16) Nojima H., Takeda-Shitaka M., Kurihara Y., Adachi M., Yoneda S., Kamiya K., Umeyama H., *Chem. Pharm. Bull.*, **50**, 1209—1214 (2002).
17) Bouvier M., Wiley D. C., *Science*, **265**, 398—402 (1994).
18) Madden D. R., Gorga J. C., Strominger J. L., Wiley D. C., *Cell*, **70**, 1035—1048 (1992).
19) Madden D. R., Wiley D. C., *Curr. Opin. Struct. Biol.*, **2**, 300—304 (1992).
20) Collins E. J., Garboczi D. N, Karpusas M. N., Wiley D. C., *Proc. Natl. Acad. Sci. U.S.A.*, **92**, 1218—1221 (1995).
21) Guo H. C., Jardetzky T. S., Garrett T. P. J., Lane W. S., Strominger J. L., Wiley D. C., *Nature* (London), **360**, 364—366 (1992).
22) Batalia M. A., Collins E. J., *Biopolymers*, **43**, 281—302 (1997).
23) Garrett T. P. J., Saper M. A., Bjorkman P. J., Strominger J. L., Wiley D. C., *Nature* (London), **342**, 692—696 (1989).
24) Saper M. A., Bjorkman P. J., Wiley D. C., *J. Mol. Biol.*, **219**, 277—319 (1991).
25) Collins E. J., Garboczi D. N., Wiley D. C., *Nature* (London), **371**, 626—629 (1994).
26) Go N., Noguti T., Nishikawa T., *Proc. Natl. Acad. Sci. U.S.A.*, **80**, 3696—3700 (1983).
27) Weiner S. J., Kollman P. A., Case D. A., Singh U. C., Ghio C., Alagona G., Profeta S. J., Weiner P., *J. Am. Chem. Soc.*, **106**, 765—784 (1984).
28) Kamiya K., Umeyama H., 19th Kozo Kassei Soukan Symposium, 1991, p. 308.
29) Kamiya K., Sugawara Y., Umeyama H., *J. Comp. Chem.*, **24**, 826—841 (2003).
30) Loncharich R. J., Brooks B. R., *Proteins*, **6**, 32—45 (1989).
31) Soejima K., Kurihara Y., Kamiya K., Umeyama H., *FEBS Lett.*, **463**, 19—23 (1999).
32) Sumikawa H., Suzuki E., Fukuhara K., Nakajima Y., Kamiya K., Umeyama H., *Chem. Pharm. Bull.*, **46**, 1069—1077 (1998).
33) Takeda-Shitaka M., Kamiya K., Miyata T., Ohkura N., Madoiwa S., Sakata Y., Umeyama H., *Chem. Pharm. Bull.*, **47**, 322—328 (1999).
34) Eckart C., *Phys. Rev.*, **47**, 552—558 (1935).